Investigations on composition and morphology of electrochemical conversion layer/titanium dioxide deposit on stainless steel

L. Bamoulid, F. Benoît-Marquié, L. Aries, A. Guenbour, A. Ben Bachir, M.-T. Maurette, F. Ansart[c] and S. El Hajjaji

Laboratoire d'Electrochimie-Corrosion, Faculté des sciences, Département de chimie, Av Ibn Batouta, BP 1014, Rabat, Morocco
Laboratoire des IMRCP, Groupe P.O.M., Université Paul Sabatier, 118 Route de Narbonne, F-31062 Toulouse, Cedex 4, France
Centre Inter-universitaire de Recherche et d'Ingénierie des Matériaux (CIRIMAT), Université Paul Sabatier, 118 Route de Narbonne, F-31062 Toulouse, Cedex 4, France

In this study, the formation and characterization of conversion coatings modified by a sol–gel TiO_2 deposit were investigated as a way to develop a new photocatalyst for water and air depollution. The conversion coating, characterised by strong interfacial adhesion, high roughness and high surface area facilitates the sol–gel deposition of titania and enhances its adhesion to the substrate. The conversion treatment is carried out in an acid solution. Observation by Scanning Electron Microscopy (SEM) reveals a rough surface with pores and cavities. According to SIMS measurements, the thickness of the initial conversion layer is evaluated at about 1.5 μm. On this pre-functionalised support, the titanium dioxide was deposited by the sol–gel method. The roughness measurements coupled with SIMS analysis allowed a precise evaluation of the surface state of the final layers. The coating consists of two layers: a TiO_2 outer layer and an inner layer containing iron chromium oxides. Characterization by X-ray diffraction (XRD) showed the existence of the TiO_2 anatase structure as the main compound.

Keywords: Conversion coating; Sol–gel; TiO_2; Stainless steel

1. Introduction

Titanium dioxide has gained extensive interest during the recent years because of its important role in various applications like photocatalysis process for water [1], [2] and [3] and air depollution [4], [5], [6] and [7]. Titania was used as a powder or deposited on a porous support. Most of the titania deposits were obtained by the sol–gel method; which presents many advantages [8] and [9]. Two conditions are necessary to have good photocatalysis system: (i) a high surface area and (ii) the main titania dioxide must be in the anatase form and must be easily accessible to the photons.

Conversion layers, obtained in an acid bath with suitable additions, can have a high surface area and a particular morphology with micropores and cavities in a large size range [10], [11] and [12]. This microstructure helps to anchor further deposits [13] and [14]. Various layers can be deposited by different methods on top of the conversion coating [10], [11], [12], [13] and [14]. In order to enhance the adhesion of the coating, thermal treatment can be carried out to induce a reaction between compounds of the conversion coating and the deposit [13] and [14].

In this investigation, a simple, inexpensive and efficient method for the deposition of thin anatase TiO_2 films on a functionalised stainless steel is presented. This method involves three steps. In the first one, the substrate surface is functionalised by a conversion treatment in an acid bath with suitable additives. In the second step, a heat treatment leads to the crystallization of the conversion coating. In the third step, titanium dioxide is deposited on the functionalised stainless steel surface by a sol–gel method. This study was undertaken to investigate the composition and morphology of the conversion coating modified by the TiO_2 deposit.

2. Experimental procedure

2.1. Material

The conversion coatings were obtained on a ferritic stainless steel (Z8C17). Substrates were in the form of 0.5 mm thick samples.

2.2. Conversion coating

Conversion coatings were obtained by chemical oxidation of the stainless steel substrate in an acid solution containing additives such as thiosulphate and propargyl alcohol in order to control the growth of the coating and to obtain a microporous morphology with high surface area. After the treatment, the samples were rinsed in demineralised water, then dried at 60 °C for 15 min. Conditions of the conversion treatment are presented in Table 2. In order to stabilise the coating, samples were treated at 450 °C for 2 h. We have chosen 450 °C for thermal treatment, because the same temperature was used for thermal treatment of TiO_2 sol–gel deposit (Table 1).

Table 1.

Conditions for the conversion treatment

Bath composition			Temperature	Treatment time
0.93 M H_2SO_4	0.005 M $Na_2S_2O_3$, 5 H_2O	0.05 M C_3H_4O	60 °C	25 min

2.3. Sol–gel process [15]

0.1 mol of titanium (IV) butoxide was dissolved in 1 mol of absolute ethanol under argon atmosphere and refluxed for 12 h. 0.05 mole of 2,4-pentanedione and 0.01 mol of double distilled water were added dropwise under vigorous stirring. After refluxing for several hours, the clear solution was concentrated by solvent distillation. An amorphous and translucid gel was obtained. It contains sufficient alcohol to avoid ageing and could therefore be stored unchanged for several weeks. The TiO_2 coating was made by a dip-coating process. The wet materials could then undergo a two-stage hot air treatment. In the first stage the catalyst system was dried at 100 °C, whereas in the second stage the desired crystalline anatase phase was obtained at 450 °C.

2.4. Characterization methods

Both secondary ion mass spectroscopy (SIMS) and X-ray diffraction (XRD) were used to analyse the coating in the initial state, after thermal treatment and deposition of titanium dioxide.

SIMS analysis was carried out using an IMS6F camera analyser. The technique gives distribution profiles of the elements across the coating. The profiles were obtained in an inert atmosphere by bombardment using cesium ion gun.

X-ray Diffraction measurements were performed using a Seifert XRD 3003-TT diffractometer equipped with secondary monochromator and with a Cu Kα radiation source ($K\alpha_1$ = 1.5405 Å and $K\alpha_2$ = 1.5455 Å) in order to reveal the nature of phases after calcinations.

Scherrer's formula was used for the calculation of crystallite sizes [8]:

$$D = \frac{0.9\lambda}{\beta\cos\theta}$$

D is the crystallites size, λ the X-ray wavelength, β the broading of the diffraction line measured at half of its maximum intensity (FWHM) and θ the corresponding angle.

The thickness of the duplex conversion coating/TiO_2 deposit has been calculated using a formula as follows:

$$e(\mu\mathrm{m}) = \frac{\Delta m}{\rho s}$$

Δm: coating weight (mg), ρ: volumic mass of anatase and s: surface of samples (cm^2).

The surface morphology was examined a scanning electron microscope (JEOL JSM 6400). B.E.T (*Brunauer–Emmet–Teller*) was used to estimate specific surface area of the coating using a formula as follows:

$$S = V_m a N / M$$

V_m

volume of gas necessary to recover the surface by one molecular layer

a

area of adsorbed molecule

N

Avogadro number = 6.02×10^{23}

M

molar volume

Surface area measurements were determined by nitrogen physisorption using a Micromeritics ASAP 2010 apparatus. All samples were degassed at 150 °C for at least 24 h prior to characterization.

3. Results and discussion

3.1. Morphology and chemical composition of the conversion coating

The initial conversion coating examined by scanning electron microscopy, before thermal treatment, presents a homogeneous surface with high roughness, formed by organized crystallites with sizes in the range of 8 to 15 μm and with a pore distribution between a few nanometers and few micrometers (Fig. 1). The main iron oxide which composes this kind of conversion coating is chromium substituted magnetite; it coexists with γ lacunar phase Fe_2O_3 type substituted by chromium to varying degrees in the surface zone [16]. The results of the secondary iron mass spectrometry (SIMS) analysis are shown in Fig. 2. The thickness of the coating evaluated by sputtering time was about 1 μm.

Fig. 1. SEM image of the initial surface of conversion coating.

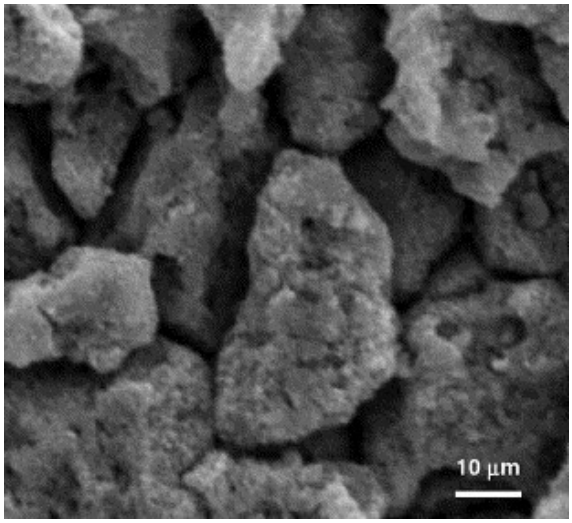

Fig. 2. Distribution profiles of elements in the initial conversion coating.

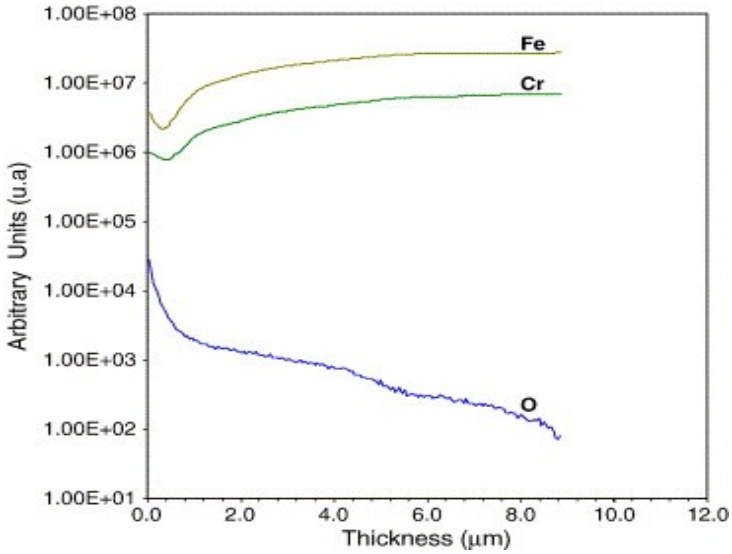

No effect of thermal treatment has been observed on the coating morphology (Fig. 3). Results of Secondary ion mass spectrometry (SIMS) analysis are presented in Fig. 4. The coating thickness increased with thermal treatment, to about 3.5 µm. In regard to the metal elements, the ion intensities continuously increase within the coating towards the metallic substrate.

Fig. 3. SEM image of the surface conversion coating after thermal treatment at 450 °C.

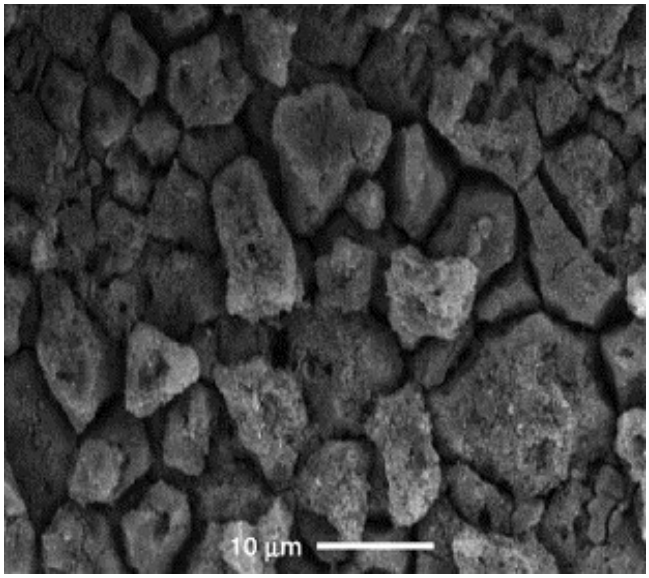

Fig. 4. Distribution profiles of elements in the conversion coating after thermal treatment at 450 °C.

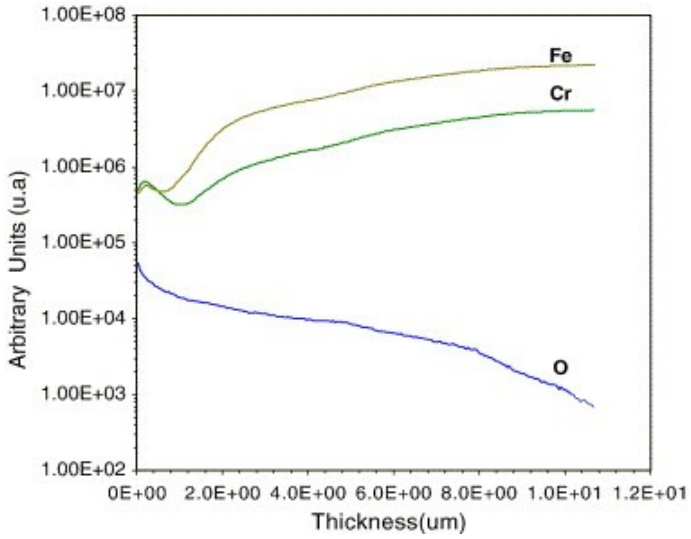

The X-ray diffraction patterns of samples heated at 450 °C is presented in Fig. 5. The peak at 22.3° is characteristic of Fe–Cr steel and is present because of the small thickness of the coating. Modifications in the coating composition were observed at this temperature; the oxygen diffuses into the coating and the oxidation of the substituted magnetite phase (which is the main coating component) leads to α-Fe_2O_3 and $FeCr_2O$

Fig. 5. X-ray diffraction patterns of iron stainless steel (1), conversion coating treated at 450 °C in air (2) and TiO_2 thin film (3). a: Fe_2O_3, b: Fe_3O_4, c: $FeCr_2O_4$ and A: anatase.

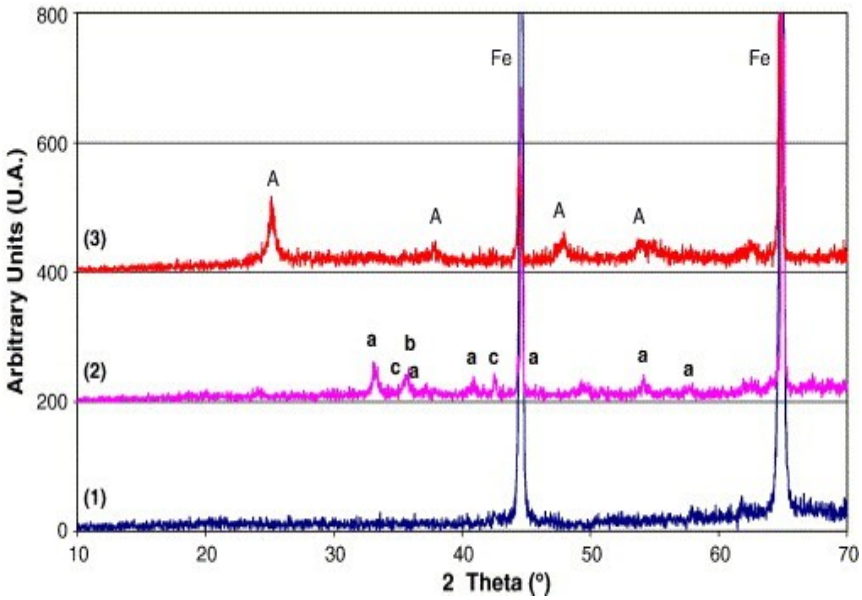

3.2. Morphology and chemical composition of the titanium dioxide coating elaborated by sol–gel process

The specific surface area measured by the BET method was about 450 m^2/m^2. The micrograph corresponding to TiO_2 deposit (Fig. 6) shows a porous structure with many chinks in the layer. The film contains numerous clusters of the TiO_2 grains measuring about 10 μm. The XRD pattern obtained for the titania layer showed that in all cases, the anatase phase of TiO_2 was obtained. XRD peaks, characteristic of anatase were observed at 2θ = 25.3°, 37°, 37.8°, 48° and 53.8° (Fig. 5).

Fig. 6. SEM image of the surface of duplex conversion coating/TiO_2 deposit.

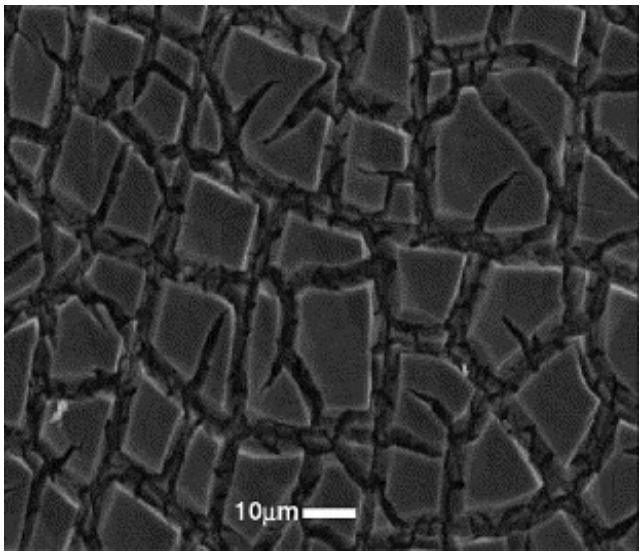

An important (101) peak of TiO_2 at $2\theta = 25.3°$ was observed. This peak corresponds to the tetragonal anatase [17] and [18]. Sizes of the TiO_2 crystallites were found to be 23.7 µm. SIMS analysis indicates very important increase on the thickness of the coating, 10 times more than thickness of the conversion coating after thermal treatment. It was estimated to be 23 µm.

Distribution profiles of the elements show that the coating can be separated in two zones; a superficial zone with a high concentration gradient and a deep zone with a low concentration gradient of TiO_2 (Fig. 7):

1— The deep layer corresponds to the primary conversion coating after thermal treatment. Profiles of iron and chromium from the conversion coating were not modified by the TiO_2. The thickness of the deep layer is the same as that of the initial conversion coating.

2— The superficial layer only contains titanium compounds deposited by the sol–gel process. The profile is continuous, which indicates a good adhesion of deposit.

Fig. 7. Distribution profiles of elements after TiO_2 deposit on conversion coating.

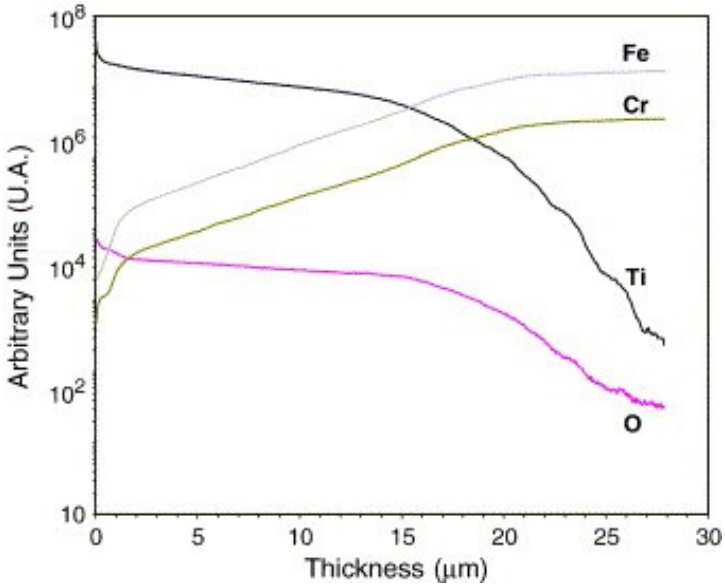

The ionic intensities change continuously within the coatings, this distribution of elements is favourable for strong deposit adhesion.

As presented in Table 2, depth of conversion coating/TiO_2 deposit increased after thermal treatment at 450 °C and is similar to the value obtained by SIMS analysis.

Table 2.

Weight and depth of substrates before and after thermal pre-treatment

Substrate with conversion coating	**Weight of conversion coating (g)**	**Weight of sol–gel coat (g)**	**Δ*m* (mg)**	**Depth (µm)**
1	2.17	2.2064	36.4	18.9
2	2.174	2.211	37	19.3
3 After thermal treatment at 450 °C	2.10	2.145	45	23

4. Conclusions

Elaboration and characterization of the system conversion layer/Titanium oxide deposit on ferritic stainless steel are presented. The conversion coating was obtained by chemical treatment in sulphuric acid bath. Thermal treatment does not significantly affect the morphology of the coating. After thermal treatment, the coating thickness increased from 1 µm to 3.5 µm. X-ray diffraction showed that the main crystallised compound induced by the thermal oxidation of the coating was hematite.

After TiO_2 deposition, the thickness of the coating significantly increases. The specific surface area measured by the B.E.T method was about 450 m^2/m^2. The superficial film contains numerous clusters of the TiO_2 grains. X-ray diffraction analysis showed that the anatase constituent is the main form of the TiO_2 obtained. SIMS analysis showed that two zones can be distinguished in the coating; the inner one, corresponding to the primary conversion coating and

the outer layer containing only TiO_2 deposited by the sol–gel process. This system will be studied as a photocatalysis support for water and air depollution.

Acknowledgment

This work was realized with the financial support within the framework of the "Action Integrée" No. MA/03/67.

References

A. Fujishima, K. Hashimoto and T. Watanabe, TiO_2 Photocatalysis: Fundamentals and Applications, Bkc Inc, Tokyo (1999).

F. Benoit-Marquié, E. Puech-Costes, A.M. Braun, E. Oliveros and M.-T. Maurette, *J. Photochem. Photobiol., A Chem.* 108 (1997), pp. 65–71.

I. Poulios, E. Micropoulou, R. Panou and E. Kostopoulou, *Appl. Catal., B Environ.* 41 (2003), p. 345.

V. Iliev, D. Tomova and L. Bilyarska, *Catal. Commun.* 5 (2004), pp. 759–763.

K. Hashimoto, *J. Phys. Chem., B* 102 (1998), p. 1724.

F. Benoit-Marquié, M.T. Boisdon, A.M. Braun, E. Oliveros and M.-T. Maurette, *Entropie* 228 (2000), pp. 36–43.

F. Benoit-Marquié, U. Wilkenhöner, V. Simon, A.M. Braun, E. Oliveros and M.-T. Maurette, *J. Photochem. Photobiol., A Chem.* 132 (2000), pp. 225–232.

R.B. Samkapal, M.Ch. Lux-Steiner and A. Ennaoui, *Appl. Surf. Sci.* 239 (2005), pp. 165–170.

E. Pelizzetti, *Solar Energy Mater. Solar Cells* 38 (1995), p. 453.

L. Ariès, F. Dabosi, INPT patent No. 9312790, 1993.

S. El Hajjaji, M.T. Maurette, E. Puech-Costes, A. Guenbour, A. Ben Bachir and L. Ariès, *Br. Corros. J.* 34 (1999), pp. 273–279.

L. Ariès and J. Roy, *Mater. Sci. Technol.* 10 (1994), p. 359.

S. El Hajjaji, A. Ben Bachir and L. Ariès, *Surf. Eng.* 17 (2001), pp. 201–204.

F. Senoq, S. El Hajjaji, J. Roy and L. Ariès, *Mater. Corros.* 51 (2000), pp. 496–501.

C. Bailleux, F. Benoît-Marquié, European patent No. 1132133, 02-03-2001.

L. Ariès, L. Albrerich, J. Roy and R. Calsou, *Br. Corr. J.* 25 (1990), p. 299.

Yu.V. Kolen'ko, B.R. Churagulov, M. Kunst, L. Mazerolles and C. Colbeau-Justin, *Appl. Catal., B Environ.* 54 (2004), pp. 51–58. View Record in Scopus | Cited By in Scopus (40)

Ha Yong lee, Y. Hwan Park and Khyun Ko, *Langmuir* 16 (2000), pp. 7289–7293.

Corresponding author. Tel./fax: +212 37 77 54 40.